A Database for II-VI & IV-VI Semiconductor Nanocrystals: Synthesis, Surface Passivation & Properties

Chantal Graafsma, BSc Thesis Chemistry, 2020

Abstract

II-VI and IV-VI semiconductor nanocrystals are among the most studied type of material in their field of research. As a result, a database serving as an extensive, yet compact source of information is highly needed. This database will focus on the synthesis, surface passivation techniques and properties of II-VI and IV-VI semiconductor nanocrystals. Through this work, scientists will be provided with an overview of the possibilities surrounding these materials, as well as given the opportunity to use this database as a recipe book for smart and efficient experiment design.

Introduction

Over the past four decades, semiconductor nanocrystals (NCs), are also referred to as quantum dots (QDs), have been studied extensively due to their extraordinary properties. Generally, QDs are particles in the nanometer regime and exhibit light-absorbing and emitting properties at room temperature as a result of quantum confinement effects. By varying the size of a QD, its band-gap can be tuned in such a way that the whole visible spectrum can be scanned using a single material. Because of these unique characteristics, NCs have been a topic of interest in a broad range of scientific fields leading to their applications in bio-imaging, energy storage, and sensors being comprehensively investigated by researchers worldwide.[1] Many different materials have been found to exhibit these properties on the nanoscale, such as II-VI, IV-VI, III-V, and perovskite type materials. Upon nanoscale dimensional reduction, their properties are found to differ significantly compared to their bulk counterparts. Due to the quantum confinement effects mentioned earlier, their properties no longer depend on the bulk material's band structure, but rather on their shape and size.[2] In order to attain desired properties from the QDs, different synthesis methods and surface treatment techniques have been developed over the past years, yielding a wide range of sizes, shapes, structural and optical properties required for their targeted applications. This work will serve as a database for syntheses, surface passivation techniques and the resulting properties of II-VI and IV-VI type QDs. Creating such a database is desirable since it will provide an overview of the possibilities this field of research offers as well as help researchers to design smart experiments to yield the desired QDs.

As mentioned above, the shape and size effect in semiconductor NCs is the result of quantum confinement. Consequently, NCs are sometimes referred to as artificial atoms and exhibit behavior similar to that of discrete atoms and molecules, such as discrete electronic transitions.[3] In bulk, semiconductor materials are characterized by their band gap energy (E_g) which is the minimum energy associated with exciting an electron from the valence band to the vacant conduction band. The interaction between the material and a photon with the required energy can cause such an excitation, leaving a hole in the valence band. This creates a hole-electron pair, referred to as the exciton. The energy to create such an exciton can be derived by solving the Hamiltonian used to describe a particle in a spherical box with infinite wall and is depicted in Eq. (1).[4]

$$E_{hv} = E_g + \frac{\hbar^2 k_{l,n}^2}{2m_e^*} + \frac{\hbar^2 k_{l',n'}^2}{2m_h^*} \qquad (1)$$

Within a semiconductor material, the formed exciton is defined by a certain size, called the Bohr exciton radius, which is varied between 1 – 200 nm depending on the material.[3] When the radius of a QD is smaller than that of the corresponding Bohr exciton radius, the material enters the quantum confinement regime, giving rise to the size effect. By differentiating the size of a QD within the quantum confinement regime, the absorbance and fluorescence emission can be tuned to the range of wavelengths desired.

The focus of this database will be on II-VI and VI-VI type materials. Semiconductor nanocrystals of II-V compounds are made up of metals from group II of the periodic table, such as zinc or cadmium, and a nonmetal from group 6, which are called chalcogens. Additionally, lead chalcogenides will also be covered, which belong to IV-VI type semiconductors. For all three metals, three chalcogens are considered, namely sulfur, selenium, and tellurium. The reason that these materials have been chosen as the focus of this database is due to the vast volume of literature available on synthetic approaches, their surface, and corresponding properties. Additionally, these materials have already been commercialized in some forms. Hence, the need to have a condensed overview of the different possibilities and challenges regarding these compounds is imperative. Compared to III-V type materials, II-VI and IV-VI semiconductors are less covalent, decreasing the need for highly reactive precursors and synthetic complexities.[5] This allows for a relatively wide range of possible approaches to the synthesis of these materials to have successful outcomes.

Within this database, three main topics related to II-VI and IV-VI QDs will be covered, namely solution-based synthesis, surface passivation and properties. Using tables, the most important synthetic parameters, surface passivation types, and the properties that arise from these techniques are depicted in a clear and straightforward manner. Using these tables, researchers can easily select the appropriate synthetic parameters and surface passivation technique required to achieve their desired QD product without the need to weed through dozens of papers first. Additionally, this work will help link the properties of different NCs to their corresponding applications.

Synthesis

Table 1: Synthetic parameters of II-VI and IV-VI type nanocrystals.

NC	Precursors	Secondary Reagents	Method	Temp.	Reaction Time	Solvent	Size	Surface Passivat-ion	PL QY	Crystal Structure
CdS[6]	R-S-S-R (R=alkyl), CdO	Oleic acid	Hot-injection	250 °C	40 min	ODE, OLA	1.8-9.4 nm	Alkane thiol capping	-	Zinc blende
CdS[7]	Cadmium stearate, TOPS	HDA	Microwave heat-up	240 °C	18 min	Decane	4.3-5.6 nm (5%)	TOP /TOPS capping	33%	Zinc blende
CdSe[8]	$Cd(Me)_2$, TOPSe	TOPO, HDA	Hot-injection	250 °C, 280 °C & 310 °C	1h, 1h & 1h	TOP	4.1 ± 0.16 nm	TOPO capping	10 - 25%	Wurtzite phase
CdSe[9]	CdO, selenium	TOPO, HDA	Hot-injection	320 °C	150s	TOPO, HDA	7.5 nm (10%)	HDA capping	85%	Wurtzite phase
CdSe[10]	$(Li)_4[Cd_{10}Se_4(SPh)_{16}]$	HDA	Heat-up	220-240 °C	100-120 min	HDA	2.5-9.0 nm	HDA capping	6 - 10%	Wurtzite phase
CdSe[11]	Cadmium stearate, TOPSe	HDA	Microwave heat-up	240 °C	1 min	Alkanes	2.5-8 nm (6%)	TOP capping	-	Wurtzite phase
CdTe[11]	Cadmium stearate, TOPTe	HDA	Microwave heat-up	220 °C	5s	Alkanes	2.5-8 nm (12%)	TOP capping	-	Zinc blende
CdTe[12]	$CdCl_2$, NaHTe	MPA	Programme process Microwave heat-up	90 °C & 100 °C	1 – 30 min	H_2O	2-4 nm	MPA capping	30 - 68.5 %	Zinc blende
CdTe[13]	CdO, TeO_2	Oleic acid, TOPO	Hot-injection	280 °C	5s – 60 min	Paraffin oil	3-8 nm (5%)	Oleic acid-capping	20 - 70%	Wurtzite phase
CdTe[14]	Cd-TDPA, Te-TBP	-	Microwave heat-up	280 °C	22 min	ODE	4.4 nm (5%)	-	-	Zinc Blende
PbS[15]	$Pb(Ac)_2$, 1-hexanethiol	-	Injection	RT	0.5 – 10h	Methanol	2-4 nm (30%)	Alkanethiol capping	-	Rock salt
PbS[16]	$Pb(CH_3COO)_3$, sodium sulfide	TGL, DTG	Injection	RT	20-80 min	H_2O	2.7 to 4.0 nm	TGL/ DTG-capping	17%	Cubic
PbS[17]	$PbCl_2$, sulfur	OLA	Hot-injection	90 °C, 220 °C	1h	OLA	6-13 nm (10%)	OLA capping	-	Rock-salt
PbS[18]	PbO, hexamethyldisilythiane	Oleic acid, TOP	Hot-injection	120 - 150 °C	1-20 min	ODE	2.6 – 6.2 nm	Oleic acid capping	59%	-
PbSe[19]	PbO, TOPSe	Oleic acid	Hot-injection	180 °C	10 – 800s	ODE	3-9 nm (7%)	Oleic acid capping	89%	Rock-salt
PbSe[20]	$PbCl_2/PbO_2$, selenium	KBH_4	Hot-injection	10 - 117 °C	1h	Alkyl-diamine	100-500 nm	Alkyl-diamine capping	-	-
PbSe[21]	$Pb(acac)_2$, selenium	Decanoic acid, OLA	Heat-up	120 °C	20 min	Paraffin oil, ODE	6.5 nm	DA/OLA capping	-	Rock-salt

PbTe[22]	PbO, TOPTe	Oleic acid	Hot-injection	140-170 °C	6 min	ODE	2.6-8.3 nm (8%)	Oleic acid capping	41-52%	Rock-salt
PbTe[21]	$Pb(acac)_2$, TOPTe	Decanoic acid, OLA	Heat-up	180 °C	20 min	Paraffin oil	8.5 nm	DA/OLA capping	-	Rock-salt
ZnS[23]	$ZnCl_2$, sulfur	PEG	Hot-injection	170 °C & 290 °C	1h	OLA	8.1 nm	OLA/PEG capping	-	Zinc blende
ZnS[17]	$ZnCl_2$, sulfur	TOPO	Heat-up	320 °C	1h	OLA	12 nm	OLA capping	1.0%	Zinc blende
ZnS[24]	Zinc stearate, thiourea, (Manganese stearate)	OLA, stearic acid	2 step hot-injection	260 °C & 240 °C	5 min & 30 min	ODE	8 nm	-	40% (Mn doping)	Cubic
ZnSe[10]	$(TMA)_4[Zn_{10}Se_4(SPh)_{16}]$	HDA	Heat-up	220-280 °C	100 - 160 min	HDA	2.8-4.8 nm (7%)	HDA capping	-	Zinc blende
ZnSe[25]	Zinc stearate, selenium	ODE	Heat-up	290 °C	1h	ODE	5.4 – 5.8 nm	Stearic acid capping	8%	Zinc blende
ZnSe[26]	$Zn(NO_3)_2$, selenium	Lithium triethylborohydride	Hot-injection	260 °C	10 - 90 min	OLA, ODE	2.6-2.9 nm	OLA-capping	-	Zinc blende
ZnSe[27]	ZnO, TOPSe	Lauric acid, HDA	Hot-injection	300 °C	5 - 40 min	Lauric acid, HDA	2.9-5.8 nm (15%)	LA/HDA capping	6.2 - 8.5%	Wurtzite
ZnSe[28]	Zinc oleate, DPPSe	DPP	Heat-up	80 - 280 °C	30 min	ODE	3.1 nm (8%)	DDP capping	72%	Zinc blende
ZnTe[29]	Zinc acetate dihydrate, TOPTe	Oleic acid, $LiBH(CH2CH_3)_3$	Hot-injection	250 °C	5 min	Benzyl ether	5 nm	TOP capping	-	Zinc blende
ZnTe[30]	Zn acetate, tellurium	$NaBH_4$, TGA	Heat-up	100 °C	7h	H_2O	5 nm	TGA capping	10%	Wurtzite

The focus of the synthesis section of this database will be on solution-based synthetic approaches. The wet synthesis of QDs has been thoroughly studied and continues to be developed further in the present day. Additionally, solution-based syntheses provide an excellent control of the surface chemistry and can easily be extracted from solution to undergo post-synthetic processing. In general, NCs grown in solution will follow the growth mechanism as proposed by LaMer.[31] This entails that for the formation of monodisperse NCs, a temporally discrete nucleation step, followed by a slower and controlled growth is required.[23] This process is represented visually in figure 1.[32]

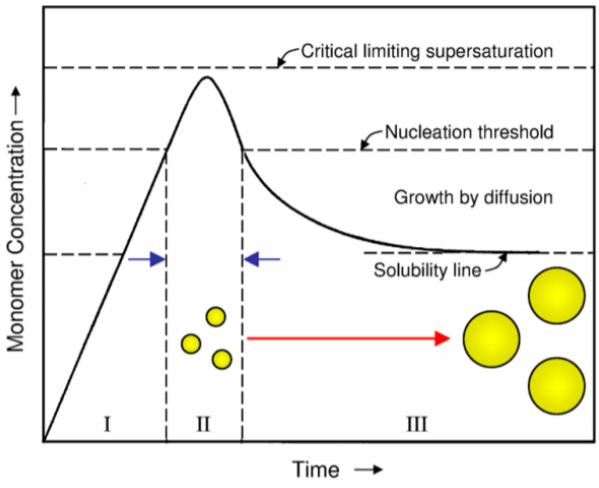

Figure 1: Schematic representation of monomer concentration during particle nucleation and growth from solution in a classical LaMer mechanism. The blue arrows identify the nucleation period (zone II). The red arrow indicates the growth period (zone III).[32]

In the table 1, three main synthetic techniques are considered, namely the hot-injection, heat-up and microwave irradiation method. For all three methods, the goal is to obtain QDs with high crystallinity, monodispersity and uniform surface composition. Hot-injection was found to be most prevalent in literature discussing syntheses of QDs. Historically, this method is also highly relevant, since it was used in one of the first successful syntheses of CdS, CdSe and CdTe QDs by Bawendi et al. in 1993.[2,33] In this method, the precursors dimethyl cadmium ($Cd(Me)_2$) and trioctylphosphine selenide (TOPSe) were injected into the coordinating solvent trioctylphosphine oxide (TOPO) at a high temperature. A representation of a simple set-up employing this method is depicted in figure 2.[34]

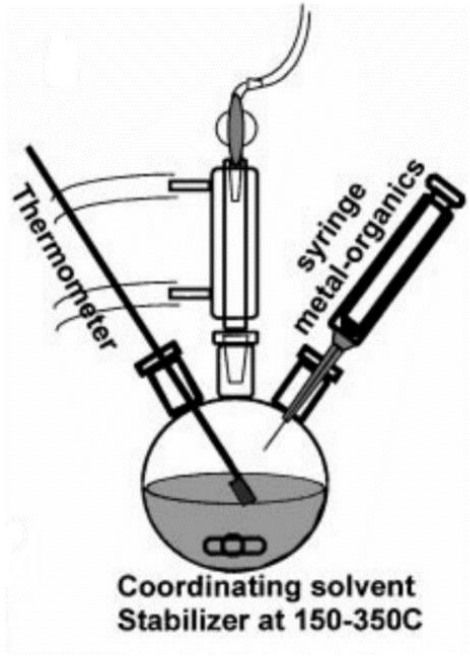

Figure 2: A simple hot-injection synthesis set-up.[34]

During the following decades, the injection method has been further developed to reduce the injection temperature and toxicity of reagents and enhance the quality and range of the formed QDs. One of the main downsides of the hot-injection method is its poor scalability and reproducability.[35] This method relies on the rapid mixing of the injected precursors, a process that slows down upon increasing the reaction volume. Furthermore, the speed at which the precursors are injected may vary between scientists and from batch-to-batch, hindering reproducibility. Due to these limitations, other synthetic methods have also been investigated, such as the heat-up method and microwave irradiation. When employing the heat-up method, all reagents are added to the reaction vessel at a low temperature. Upon heating the reaction, the precursors will increasingly form monomers and eventually the nucleation of crystallites will take place. During the growth process of the NCs, heating is continued until the desired product is formed. One of the main challenges of the heat-up approach is the necessity to select the precursors more carefully compared to injection methods. The chosen precursors should yield rapid nucleation to ensure that large quantities of nanosized nuclei are formed quickly, as well as ensure decoupling of the nucleation and growth stages to enhance monodispersity.[35] Similar to the heat-up method, microwave irradiation also provides enhanced control of the reaction temperature and pressure. Using microwave irradiation, precursor solutions can be heated more rapidly compared to the conventional heat-up method. Furthermore, interactions between the precursors, intermediates or formed QDs and the electromagnetic field can play a large role in the reaction mechanism, giving rise to opportunities that cannot be achieved using conventional methods.[36]

Besides using the right synthesis method, choosing appropriate precursors is also crucial to the successful synthesis of QDs. Over the years, many different precursors have been employed and evaluated, each having their own advantages and drawbacks. Here, the most important types of precursors will be briefly discussed. In the ground-breaking method developed by Bawendi et al., the precursor $Cd(Me)_2$ was used as the metal source. This method using organometallic precursors was further developed in the following years, yielding good results.[8,33] However, $Cd(Me)_2$ is highly toxic and air sensitive. Furthermore, this synthesis requires TOPO as a solvent, which must be heated to high temperatures (300 °C) and above its flashpoint.[2] Overall, these conditions are less than

ideal and have driven scientists to look for alternative methods without employing these hazardous and expensive compounds. Alternatives to organometallic precursors include metal carboxylates, metal oxides, and metal salts. The presence of a strong acid or anion in the metal precursor allows for the synthesis of high quality NCs with reduced risks and costs.[37] However, these syntheses often still require an inert atmosphere and high temperatures. Alternatively, single-source precursors have also attracted the attention of researchers over the past decades. As the name suggests, single-source precursors function as the source for both the metal and chalcogen in the synthesis of QDs. For example, metal salts of alkylxanthates can be used under atmospheric conditions at lower temperatures to synthesize QDs.[38] Furthermore, inorganic metal-chalcogenide clusters in an alkylamine solvent can be used to synthesize organically passivated, spherical QDs on a large scale.[10]

Choosing the right synthetic parameters has proven to be crucial when promoting reproducibility and scalability as well as reducing cost and risks. However, the parameters of a synthesis can also significantly affect the shape, size, and crystal structure of the final QD product. This database focusses mainly on spherical QDs, however, it has been found that shape control can be achieved by tuning the synthetic parameters. In a study by Guo et al., the different reactivities of a series of dialkyl dichalcogenides yield a wide range of morphologies, such as spheres, rods and multipods.[6] Furthermore, the presence and concentration of secondary reagents and capping agents, such as superhydride and oleylamine (OLA) can also be tuned to gain control over the shape of QDs.[26,29] The size of NCs is usually controlled through the reaction time, as is exhibited by many different synthetic approaches.[13,19,27] This phenomenon is illustrated in figure 3.[13] Not only the size and shape, but also the crystal structure of a QD can be controlled by careful experiment design. It has been found that the formed crystals structure within a QD is dependent on the growth temperature, with cubic structures being favored at lower temperatures whereas higher temperatures will yield the wurtzite structure.[13,39]

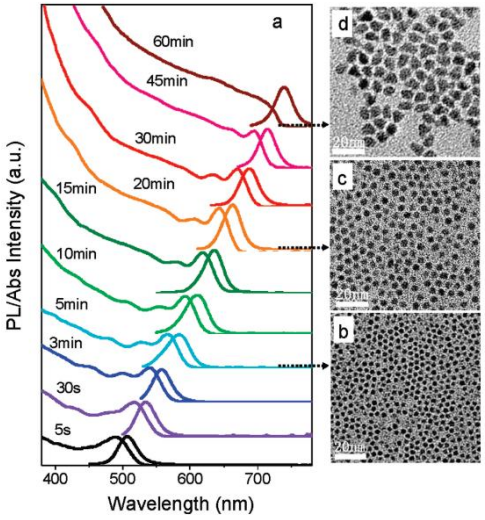

Figure 3: (a) Temporal evolution of the UV-vis absorption and photo-luminescence spectra of CdTe nanocrystals. TEM images of CdTe nanocrystals with an average diameter of: (b) 3.4 , (c) 4.5, and (d) 8.6 nm.[13]

Surface Passivation

Table 2: Synthetic parameters and properties of core/shell nanocrystals.

NC	Type	Lattice Mis-match	Precursors	Secondary Reagents	Method	Temp.	Reaction Time	Solvent	Size	PL QY	Crystal Structure
CdS/ZnS[40]	Type I	7.5%[41]	Cadmium stearate, sulfur, zinc ethylxanthate	OLA, Oleic acid, TOP	Hot-injection	300 °C & 225 °C	20 min & 45 min	ODE	6.8 nm	41%	Wurtzite
CdSe/CdS[42]	Type I	3.9%[43]	Cadmium-myristic acid, selenourea, thiourea	Oleic acid	Heat-up	180 °C & 140 °C	15-22 min & 4h	Toluene & H_2O	2.8 nm	60 - 80%	Cubic
CdSe/ZnS[44]	Type I	10.6%[43]	CdO, TOPSe, zinc acetate, octanethiol	ODPA, Oleic acid	Hot-injection	300 °C	2 min & 20-60 min	TOA	4 nm ± 0.5 nm	53 – 62%	Hexagonal
CdSe/ZnSe[43,45]	Type II	6.3%	CdO, selenium, zinc stearate, TOPSe	DPA	Hot-injection	250 °C & 200 °C		TOPO, HDA	4.6 nm (5%)	85%	-
$Cd_{1-x}Zn_xSe/ZnS$[46]	Type I	-	cadmium stearate, zinc stearate, TOPSe, zinc ethylxanthate	OLA, ODE	Hot-injection	310 °C & 210 °C	20 min & 1h	OLA, ODE	4.4 nm	67%	Wurtzite
CdTe/CdS[47]	Type II	10.2%	$CdCl_2$, NaHTe	TGA	Heat-up & illumination	100 °C	20 min & 20 days	H_2O	-	85%	Cubic
ZnSe/ZnS[48]	Type I	4.4%[49]	Diethylzinc, TOPSe, zinc oleate, 1-octanethiol	TOP, ODE	Hot-injection	295°C, 240°C	30 min & 5 min	OLA, oleic acid	5.4 nm	85 %	Zinc-blende
PbSe/CdSe[50]	Type I	~1%	PbO, TOPSe, CdO	Oleic acid	Hot-injection	205 °C & 100 °C	100s	TOP, phenyl ether & ODE	5-7 nm	20-30%	Rock salt & zinc blende
PbSe/CdSe/ZnS[50]	Type I	1% & 10.6%	PbO, TOPSe, CdO, diethyl zinc, hexamethyl disilathiane	Oleic acid, TOP	Hot-injection	205 °C & 100 °C	25s, 19.5h & 22 min	Phenyl ether & ODE	5.7 nm	50%	Cubic
$PbSe/PbSe_xS_{1-x}$[51,52]	Type II	1.3%	Lead acetate, TOPSe, TOPS	Oleic acid	Hot-injection	180 °C	15 min	Diphenyl ether	6.7 nm	65%	Rock salt

Aside from synthesizing QDs which are made up of only one material, it is also possible to form core/shell type structures, as is shown in the table above. Forming an inorganic shell around a QD is an excellent way to passivate its surface and improve its optical properties. By passivating the surface of a QD, surface trap states that can arise from dangling bonds are combatted, enhancing the photoluminescence quantum yield (PL QY). Besides this, an inorganic shell also acts as a physical barrier between the optically active core and environmental changes and photo-oxidation.[53] Generally, the synthesis of core/shell QDs takes place in two steps. First, the core is synthesized similarly to the synthesis of core only QDs, as described in the previous section. In the second step, different precursors are used to form a shell structure around the core through epitaxial-type shell growth. Core/shell QDs can be classified by considering the band-gap of their bulk materials, as is visualized in figure 4.[53]

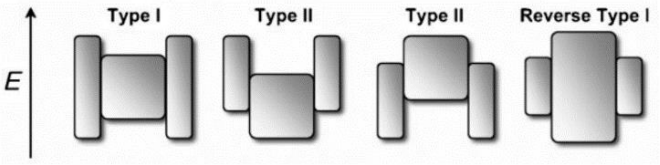

Figure 4: Band-gap structure of different core/shell QD materials.[53]

In type I core/shell QDs, the band-gap of the shell material is larger than that of the core. Consequently, both the electrons and holes are confined in the core material. Type I core/shell QDs typically have improved optical properties and allow the optically active core to be shielded from harmful environmental factors such as air and water. For type II core/shell QDs, either the conduction-band edge or the valence-band edge or the shell is located in the band-gap of the core material. As a result, the separation of holes and electrons within the core/shell structure occurs. Generally, a significant red-shift is observed for type II core/shell QDs. By controlling the shell thickness, the emission wavelength can be tuned, which can be desirable for certain applications. A downside to type II core/shell QDs is that they generally have a reduced stability and PL QY. For reverse type I QDs, the band-gap of the core is larger than that of the shell, causing the electrons to be either partially or completely confined in the shell, depending on its thickness. [53]

It is clear that in order to successfully design a core/shell QD, the band-gap of both the shell and core are to be considered. Furthermore, the crystal structure of the core and shell material must also be taken into account in order to ensure a smooth, low-defect interface between the two layers.[50] If defects occur at the core-shell interface, these can act as trap states, reducing the optical properties of the QD. This requirement can be evaluated by considering the lattice parameter mismatch, which gives an indication of the difference between the two crystal structures. If the lattice parameter mismatch between two materials is especially large, the strain arising from this could be battled through a gradient between the two layers instead of a harsh transition, as was found for CdSe/ZnS core/shell QDs.[44] Furthermore, it is also possible to use alloyed semiconductor materials as the cores or shell, giving rise to additional and tunable properties. [46,51]

Arguably, one of the most important properties to control when synthesizing core/shell QDs is the thickness of the shell. The formed shell must be thick enough to properly passivate the surface and protect the core, but thin enough so that the strain and crystal defects induced by the lattice parameter mismatch do not diminish the PL QY. Furthermore, control over the shell thickness is necessarily when tuning the optical properties of type II core/shell QDs. To ensure controlled growth of the shell, the temperature at which it is grown is generally lower than the reaction temperature of the core, and precursors are added slowly. Additionally, the composition of the core must be known to accurately calculate the amount of precursors necessary to achieve the desired shell thickness.[53]

Table 3: Common ligands and their properties.

Ligand	Chemical Structure	Binding Type[54]	Nanocrystal Examples	Binding Mode	PL QY	Notes
Trioctylphosphine oxide (TOPO)	$OP(C_8H_{17})_3$	L-Type (?)	CdSe[55] CdSe/ZnS[56]	O-Cd	3.5%[57] 40%	
Trioctylphosphine (TOP)	$P(C_8H_{17})_3$	L-Type	CdSe[55]	P-Se	50%[58]	For Se-rich CdSe
Hexadecylamine (HDA)	$C_{16}H_{35}N$	L-Type	CdSe[9]		85%	
Dodecylamine (DDA)	$C_{12}H_{27}N$	L-Type	CdSe[59] CdTe[59]	N-Cd & N-Se	15–20% 30–65%	
Oleylamine (OLA)	$C_{18}H_{37}N$	L-Type	PbS[60] CdTe[61] ZnSe[26]		40% 20%	
$InCl_3$	-	Z-Type	CdTe[61] CdSe[61]	In-Te In-Se	90% 11.5%	
$CdCl_2$	-	Z-Type	CdTe[61]	Cd-Te	73%	
Tetrabutylammonium chloride (TBACl)	$[CH_3(CH_2)_3]_4NCl$	X-Type	CdTe[61]	Cl-Cd	28%	
Oleic Acid	$C_{18}H_{34}O_2$	X-Type	PbS[62] PbSe[19] CdTe[13]		90% 89% 70%	
Stearic acid	$C_{18}H_{36}O_2$	X-Type	ZnSe[25]		8%	
3-Mercaptopropionic acid (MPA)	$HSCH_2CH_2CO_2H$	X-Type	CdSe/ZnS[56] CdTe[12]	S-Zn & S-S	42% 68.5%	Useful for transferring NCs to aqueous solution
Alkyl thiols	R-SH	X-Type	CdS[63] CdSe/ZnS[56]	S-Zn & S-S		

A different way to tackle surface trap states is through the use of (organic) ligands. Ligands are molecules that are bound to the surface of QDs. They can act as stabilizing agents by providing colloidal stability, and stopping unwanted growth and agglomeration.[55] Besides this, their electronic structure plays an important role in the optical properties of QDs through their interaction with surface states. Capping ligands on the surface of QDs can either be a direct effect of the reagents and solvents used in their syntheses or can be the result of post-synthetic surface treatments. The most important ligands and their characteristics are shown in the table 3.

The classification of ligands is commonly done through the covalent bond classification (CBC), which was proposed by Green et al.[54] Firstly, there are L-type ligands which bind like neutral two-electron donors and are therefore Lewis bases. Ligands such as amines and phosphines belong to this class. The second class of ligands are called Z-type and bind by accepting two electrons. These are known as Lewis acids and include metal halides and metal carboxylates. Finally, X-type ligands bind by sharing one electron with a singly occupied orbital on the surface of the QD and therefore form a covalent bond. X-type ligands include thiols and carboxylic acids.

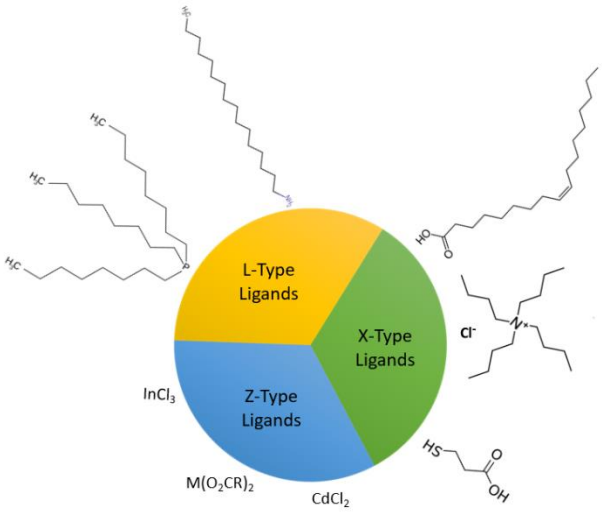

Figure 5: An overview of a selection of different ligands classified according to the CBC.

From studies on post-synthetic surface treatment of QDs with passivating ligands, it was found that Z-type ligands are especially good at passivating anionic surface trap states.[61] In this study, a massive increase in PL QY up to 90% was found without the need to grow a passivating inorganic shell, but upon treatment of CdTe QDs with $InCl_3$ and $CdCl_2$.

Organic ligands can also be extremely useful to improve the properties of QDs. For example, it was found that the PL QY of QDs synthesized in a TOPO-TOP mixture could be improved up to 70% by subsequent treatment with primary amines.[59] Upon the exchange of TOP with primary amines, the type of ligands remains the same, namely L-type. However, the increase in optical properties can be explained by looking at the structures of the two different ligands. Primary amines are less sterically hindered and therefore have a better surface coverage and thus an enhanced passivation of surface trap states.[55]

Besides just improving the optical properties of QDs, ligands can also improve stability for storage and processing. This can be especially useful when transferring QDs synthesized in organic solvents to aqueous media is required for their specific applications. 3-Mercaptopropionic acid (MPA) can be used to replace TOPO ligands in CdSe/ZnS core/shell QD at room temperature.[56] After the ligand exchange, the QDs could be transferred to an aqueous environment without a significant loss of PL QY and with good colloidal stability, giving rise to new possibilities with regards to applications.

Properties

Table 3: Properties of II-VI and IV-VI type nanocrystals.

NC	Type	Bulk bandgap (eV)[53]	Bulk crystal structure[53]	Lattice parameter (Å)[53]	Bohr radius (nm)	PL QY	FWHM
CdS	II-VI	2.49	Wurtzite	4.14/6.71	2.5-3.0[6]	33%[7]	24 nm
CdSe	II-VI	1.74	Wurtzite	4.3/7.01	5.4[6]	85%[9]	23 nm
CdTe	II-VI	1.43	Zinc blende	6.48	7.5[64]	70%[13]	28 nm
PbS	IV-VI	0.41	Rock salt	5.94	18[65]	59%[18]	-
PbSe	IV-VI	0.28	Rock salt	6.12	46[65]	89%[19]	145 nm
PbTe	IV-VI	0.31	Rock salt	6.46	46[66]	52%[22]	130 meV
ZnS	II-VI	3.61	Zinc blende	5.41	2.5[67]	40%[24]	-
ZnSe	II-VI	2.69	Zinc blende	5.67	4.5[68]	72%[28]	22 nm
ZnTe	II-VI	2.39	Zinc blende	6.10	6.2[29]	10%[30]	-

After synthesizing QDs or performing post-synthetic surface treatments on them, there are several properties that must be considered when analyzing the final product. Arguably the most important property to take into account when evaluating the quality of the formed NCs, is the photoluminescence quantum yield (PL QY). This property is a measure of the efficiency of the optical properties of a NC and is defined as the number of photons emitted as a percentage of the number of photons absorbed. As discussed earlier, the PL QY of a QD can be negatively affected by the formation of surface trap states and defects in its crystal structure. Therefore, evaluating how the PL QY changes when different synthetic techniques and surface treatments are employed can provide information on how effective they are with regards to achieving high crystallinity and passivating surfaces. Furthermore, a high PL QY is often required for optoelectronic applications including displays, LEDs and bioimaging.[48] QDs are a promising class of materials for LEDs, since they can provide high lightning efficiency by directly converting an electrical current into a stream of photons at low production costs. Figure 6 shows the band structure of an inverted QD-LED in which the emitting layer is based on a CdSe/$CdSe_xS_{1-x}$/CdS core/shell/shell QD structure.[69]

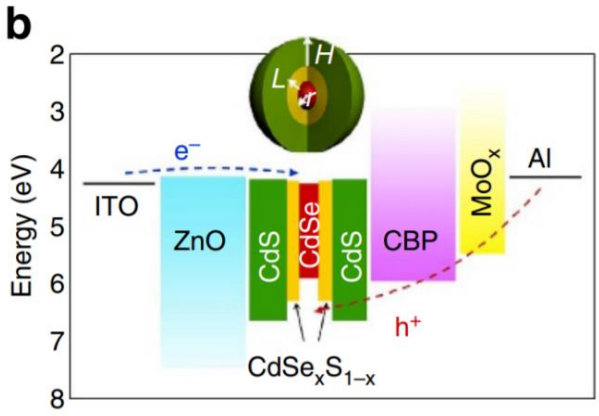

Figure 6: Energy band diagram of the inverted QD-LED with an active emitting layer based on CdSe/$CdSe_xS_{1-x}$/CdS QDs with an alloyed interface.[69]

Besides the PL QY, it is also important to consider the full width at half maximum (FWHM) of the photoluminescence spectra of QDs. This value gives an indication of the size distribution of the sample, with a small FWHM corresponding to a narrow size distribution of the QDs.[9] Monodispersity is an important goal when synthesizing QDs and synthesis is often followed by a second step in which the QDs are separated based on their size. This technique employs the size

dependent stability of the QDs in different solvents to extract a narrow size distribution.[4] However, synthetic techniques that yield a narrow size distribution directly are preferred, since this will increase the yield of the reaction and reduce processing costs. Besides the FWHM, transmission electron microscopy imaging can also be used to determine the monodispersity of the synthesized NCs.[19]

In order to successfully implement the use of NCs in applications, there is a third property that is of extreme importance, namely its colloidal stability. Unlike the PL QY and FWHM, colloidal stability is difficult to quantify, since it is dependent on the solvent, temperature, and pH for aqueous environments. Furthermore, surface chemistry plays a major role and must be thoroughly understood to predict long-term stability. For example, organic ligands such as OLA can provide good colloidal stability in apolar solvents.[60] However, inorganic ligands such as halides, chalcogenidometallates, and oxometallates in turn generally provide good colloidal stability in polar solutions. Furthermore, inorganically capped NCs are especially well suited for applications in solar cells and photodetectors, since they do not block electron transfer.[1] One application in which colloidal stability and solubility is especially important is in bioimaging. In order to use NCs for biological applications, post-synthetic surface treatments are usually employed to ensure stability and solubility in aqueous solutions without reducing the PL QY drastically. Furthermore, applications in sensing and detecting require the fluorescence properties of the NC to remain relatively unaffected by the environmental pH.[56] Overall, solubilization of NCs in aqueous solution is a domain in which much progress is still expected.[70] Besides stability and solubility, the organic ligands on NCs used for biomedical applications can also provide functionality for specific targeting, reducing interactions with the immune system, and providing contrast for imaging. In these kinds of applications, NCs can be used as theranostics, which are platforms in which diagnostics are combined with subsequent treatment.[1]

Outlook & Conclusions

Although the scientific community surrounding semiconductor nanocrystals has seen many breakthroughs over the past four decades, this field of research is currently still being developed. An increasing amount of effort is being made to find earth-abundant and non-toxic materials that exhibit the same stability and optical properties as their cadmium- and lead-based counterparts. While III-V type QDs are a promising class of materials, their covalent nature compared to II-VI and IV-VI type QDs results in the need more complex syntheses. Furthermore, their low PL QY in aqueous environments has also been a major obstacle.[71] Lately, a transition from binary II-VI & VI-VI to ternary I-III-VI_2 and quaternary I_2-II-IV-VI_4 metal chalcogenides has been observed. These materials with higher complexities are a response to the growing demand for highly optimized optoelectronics.[1] The properties of QDs can also be further tuned through doping. By introducing small amounts of dopants, additional characteristics such as large Stokes shifts, paramagnetic properties, and improved lasing can be introduced.[3]

The major challenges in using QDs in applications are their long-term colloidal stability coupled with the loss or decrease of optoelectronic properties during processing steps. Furthermore, *in situ* observation of NC formation at the nucleation stage and at the very early stage of growth remains a major barrier in fully understanding the mechanism of NC synthesis.[1] Overall, there are many opportunities and challenges that remain to be tackled within this field of research.

In conclusion, it has become apparent that there are many aspects to consider when studying the field of research focusing on II-VI and IV-VI QDs. In order to successfully produce NCs with desired properties, an understanding of the theory surrounding the synthetic techniques and post-synthetic surface treatments is key. This database can help provide an overview of the many factors that contribute to shaping the properties of QDs. By ensuring that the database is kept up to date with new breakthroughs, as well as by expanding it to include more types of materials, such as III-V, perovskite, doped, ternary and quaternary NCs, it can serve as an extensive yet compact source of information, helping scientists to design their experiments in a smart and efficient manner.

References

1. Kovalenko, M. V. *et al.* Prospects of nanoscience with nanocrystals. *ACS Nano* **9**, 1012–1057 (2015).

2. Gun'ko, Y. K. & Byrne, S. *Quantum dot synthesis methods*. *Quantum Dot Sensors: Technology and Commercial Applications* vol. 5 (2012).

3. Smith, A. M. & Nie, S. Semiconductor nanocrystals: Structure, properties, and band gap engineering. *Acc. Chem. Res.* **43**, 190–200 (2010).

4. Bawendi, M. G. Synthesis and Spectroscopy of II–VI Quantum Dots: An Overview. 339–356 (1995) doi:10.1007/978-1-4615-1963-8_12.

5. Livache, C., Martinez, B., Goubet, N., Ramade, J. & Lhuillier, E. Road map for nanocrystal based infrared photodetectors. *Front. Chem.* **6**, 1–11 (2018).

6. Guo, Y., Alvarado, S. R., Barclay, J. D. & Vela, J. Shape-programmed nanofabrication: Understanding the reactivity of dichalcogenide precursors. *ACS Nano* **7**, 3616–3626 (2013).

7. Washington, A. L. & Strouse, G. F. Microwave synthetic route for highly emissive TOP/TOP-S passivated CdS quantum dots. *Chem. Mater.* **21**, 3586–3592 (2009).

8. Talapin, D. V., Rogach, A. L., Kornowski, A., Haase, M. & Weller, H. Highly Luminescent Monodisperse CdSe and CdSe/ZnS Nanocrystals Synthesized in a Hexadecylamine-Trioctylphosphine Oxide-Trioctylphospine Mixture. *Nano Lett.* **1**, 207–211 (2001).

9. Qu, L. & Peng, X. Control of photoluminescence properties of CdSe nanocrystals in growth. *J. Am. Chem. Soc.* **124**, 2049–2055 (2002).

10. Cumberland, S. L. *et al.* Inorganic clusters as single-source precursors for preparation of CdSe, ZnSe, and CdSe/ZnS nanomaterials. *Chem. Mater.* **14**, 1576–1584 (2002).

11. Washington, A. L. & Strouse, G. F. Microwave synthesis of CdSe and CdTe nanocrystals in nonabsorbing alkanes. *J. Am. Chem. Soc.* **130**, 8916–8922 (2008).

12. He, Y. *et al.* Synthesis of CdTe nanocrystals through program process of microwave irradiation. *J. Phys. Chem. B* **110**, 13352–13356 (2006).

13. Shen, H. *et al.* Size-and shape-controlled synthesis of CdTe and PbTe nanocrystals using tellurium dioxide as the tellurium precursor. *Chem. Mater.* **22**, 4756–4761 (2010).

14. Song, Q. *et al.* Microwave-assisted synthesis of monodispersed CdTe nanocrystals. *Chem. Commun.* **46**, 4971–4973 (2010).

15. Chen, S., Truax, L. A. & Sommers, J. M. Alkanethiolate-protected PbS nanoclusters: Synthesis, spectroscopic and electrochemical studies. *Chem. Mater.* **12**, 3864–3870 (2000).

16. Bakueva, L. *et al.* PbS quantum dots with stable efficient luminescence in the near-IR spectral range. *Adv. Mater.* **16**, 926–929 (2004).

17. Joo, J. *et al.* Generalized and facile synthesis of semiconducting metal sulfide nanocrystals. *J. Am. Chem. Soc.* **125**, 11100–11105 (2003).

18. Lingley, Z., Lu, S. & Madhukar, A. A high quantum efficiency preserving approach to ligand exchange on lead sulfide quantum dots and interdot resonant energy transfer. *Nano Lett.* **11**, 2887–2891 (2011).

19. Yu, W. W., Falkner, J. C., Shih, B. S. & Colvin, V. L. Preparation and characterization of monodisperse

PbSe semiconductor nanocrystals in a noncoordinating solvent. *Chem. Mater.* **16**, 3318–3322 (2004).

20. Lifshitz, E. *et al.* Synthesis and characterization of PbSe quantum wires, multipods, quantum rods, and cubes. *Nano Lett.* **3**, 857–862 (2003).

21. Niu, J. *et al.* Controlled synthesis of high quality PbSe and PbTe nanocrystals with one-pot method and their self-assemblies. *Colloids Surfaces A Physicochem. Eng. Asp.* **406**, 38–43 (2012).

22. Murphy, J. E. *et al.* PbTe colloidal nanocrystals: Synthesis, characterization, and multiple exciton generation. *J. Am. Chem. Soc.* **128**, 3241–3247 (2006).

23. Quan, Z., Wang, Z., Yang, P., Lin, J. & Fang, J. Synthesis and characterization of high-quality ZnS, ZnS:Mn2+, and ZnS:Mn2+/ZnS (Core/Shell) luminescent nanocrystals. *Inorg. Chem.* **46**, 1354–1360 (2007).

24. Jana, S., Srivastava, B. B. & Pradhan, N. A controlled growth process to design relatively larger size semiconductor nanocrystals. *J. Phys. Chem. C* **117**, 1183–1188 (2013).

25. Banski, M. *et al.* Special Role for Zinc Stearate and Octadecene in the Synthesis of Luminescent ZnSe Nanocrystals. *Chem. Mater.* **27**, 3797–3800 (2015).

26. Chen, W. *et al.* Spontaneous shape and phase control of colloidal ZnSe nanocrystals by tailoring Se precursor reactivity. *CrystEngComm* **21**, 2955–2961 (2019).

27. Chen, H. S. *et al.* Colloidal ZnSe, ZnSe/ZnS, and ZnSe/ZnSeS quantum dots synthesized from ZnO. *J. Phys. Chem. B* **108**, 17119–17123 (2004).

28. Yu, K. *et al.* Highly-photoluminescent ZnSe nanocrystals via a non-injection-based approach with precursor reactivity elevated by a secondary phosphine. *Chem. Commun.* **47**, 8811–8813 (2011).

29. Zhang, J., Sun, K., Kumbhar, A. & Fang, J. Shape-control of ZnTe nanocrystal growth in organic solution. *J. Phys. Chem. C* **112**, 5454–5458 (2008).

30. Cheng, T. *et al.* Aqueous synthesis of high-fluorescence ZnTe quantum dots. *J. Mater. Sci. Mater. Electron.* **26**, 4062–4068 (2015).

31. Lamer, V. K. & Dinegar, R. H. Theory, Production and Mechanism of Formation of Monodispersed Hydrosols. *J. Am. Chem. Soc.* **72**, 4847–4854 (1950).

32. Wang, F., Richards, V. N., Shields, S. P. & Buhro, W. E. Kinetics and mechanisms of aggregative nanocrystal growth. *Chem. Mater.* **26**, 5–21 (2014).

33. Murray, C. B., Norris, D. J. & Bawendi, M. G. Synthesis and Characterization of Nearly Monodisperse CdE (E = S, Se, Te) Semiconductor Nanocrystallites. *J. Am. Chem. Soc.* **115**, 8706–8715 (1993).

34. Murray, C. B., Kagan.R., and B. M. G. Synthesis and Characterization of Monodisperse Nanocrystals and Close-Packed Nanocrystal Assemblies. *Annu. Rev. Mater. Sci.* **30**, 545–610 (2006).

35. Van Embden, J., Chesman, A. S. R. & Jasieniak, J. J. The heat-up synthesis of colloidal nanocrystals. *Chem. Mater.* **27**, 2246–2285 (2015).

36. Baghbanzadeh, M., Carbone, L., Cozzoli, P. D. & Kappe, C. O. Microwave-assisted synthesis of colloidal inorganic nanocrystals. *Angew. Chemie - Int. Ed.* **50**, 11312–11359 (2011).

37. Qu, L., Peng, Z. A. & Peng, X. Alternative Routes toward High Quality CdSe Nanocrystals. *Nano Lett.* **1**, 333–337 (2001).

38. Pradhan, N. & Efrima, S. Single-precursor, one-pot versatile synthesis under near ambient conditions of tunable, single and dual band fluorescing metal sulfide nanoparticles. *J. Am. Chem. Soc.* **125**, 2050–2051 (2003).

39. Jun, Y. W., Lee, S. M., Kang, N. J. & Cheon, J. Controlled synthesis of multi-armed CdS nanorod architectures using monosurfactant system. *J. Am. Chem. Soc.* **123**, 5150–5151 (2001).

40. Protière, M. & Reiss, P. Facile synthesis of monodisperse ZnS capped CdS nanocrystals exhibiting efficient blue emission. *Nanoscale Res. Lett.* **1**, 62–67 (2006).

41. Little, R. B., El-Sayed, M. A., Bryant, G. W. & Burke, S. Formation of quantum-dot quantum-well heteronanostructures with large lattice mismatch: ZnS/CdS/ZnS. *J. Chem. Phys.* **114**, 1813–1822 (2001).

42. Pan, D., Wang, Q., Jiang, S., Ji, X. & An, L. Synthesis of extremely small CdSe and highly luminescent CdSe/CdS core-shell nanocrystals via a novel two-phase thermal approach. *Adv. Mater.* **17**, 176–179 (2005).

43. Reiss, P., Bleuse, J. & Pron, A. Highly Luminescent CdSe/ZnSe Core/Shell Nanocrystals of Low Size Dispersion. *Nano Lett.* **2**, 781–784 (2002).

44. Jun, S. & Jang, E. Interfused semiconductor nanocrystals: Brilliant blue photoluminescence and electroluminescence. *Chem. Commun.* **1**, 4616–4618 (2005).

45. Reiss, P., Carayon, S. & Bleuse, J. Large fluorescence quantum yield and low size dispersion from CdSe/ZnSe core/shell nanocrystals. *Phys. E Low-Dimensional Syst. Nanostructures* **17**, 95–96 (2003).

46. Protière, M. & Reiss, P. Highly luminescent Cd1-xZnxSe/ZnS core/ shell nanocrystals emitting in the blue-green spectral range. *Small* **3**, 399–403 (2007).

47. Bao, H., Gong, Y., Li, Z. & Gao, M. Enhancement effect of illumination on the photoluminescence of water-soluble CdTe nanocrystals: Toward highly fluorescent CdTe/CdS core-shell structure. *Chem. Mater.* **16**, 3853–3859 (2004).

48. Ji, B., Koley, S., Slobodkin, I., Remennik, S. & Banin, U. ZnSe/ZnS Core/Shell Quantum Dots with Superior Optical Properties through Thermodynamic Shell Growth. *ACS Appl. Mater. Interfaces* (2020) doi:10.1021/acs.nanolett.9b05020.

49. Gheshlaghi, N., Pisheh, H. S., Karim, M. R. & Ünlü, H. Interface Strain Effects on ZnSe/ (CdSe) based Type i and ZnSe/CdS Type II Core/Shell Quantum Dots. *Energy Procedia* **102**, 152–163 (2016).

50. Pietryga, J. M. *et al.* Utilizing the lability of lead selenide to produce heterostructured nanocrystals with bright, stable infrared emission. *J. Am. Chem. Soc.* **130**, 4879–4885 (2008).

51. Lifshitz, E. *et al.* Air-stable PbSe/PbS and PbSe/PbSexS1-x Core - Shell nanocrystal quantum dots and their applications. *J. Phys. Chem. B* **110**, 25356–25365 (2006).

52. Brumer, M. *et al.* PbSe/PbS and PbSe/PbSexS1-x core/shell nanocrystals. *Adv. Funct. Mater.* **15**, 1111–1116 (2005).

53. Reiss, P., Protière, M. & Li, L. Core/shell semiconductor nanocrystals. *Small* **5**, 154–168 (2009).

54. Green, M. L. H. A new approach to the formal classification of covalent compounds of the elements. *J. Organomet. Chem.* **500**, 127–148 (1995).

55. Green, M. The nature of quantum dot capping ligands. *J. Mater. Chem.* **20**, 5797–5809 (2010).

56. Pong, B. K., Trout, B. L. & Lee, J. Y. Modified ligand-exchange for efficient solubilization of CdSe/ZnS

quantum dots in water: A procedure guided by computational studies. *Langmuir* **24**, 5270–5276 (2008).

57. Bullen, C. & Mulvaney, P. The effects of chemisorption on the luminescence of CdSe quantum dots. *Langmuir* **22**, 3007–3013 (2006).

58. Jasieniak, J. & Mulvaney, P. From Cd-rich to Se-rich - The manipulation of CdSe nanocrystal surface stoichiometry. *J. Am. Chem. Soc.* **129**, 2841–2848 (2007).

59. Talapin, D. V. *et al.* Synthesis and surface modification of amino-stabilized CdSe, CdTe and InP nanocrystals. *Colloids Surfaces A Physicochem. Eng. Asp.* **202**, 145–154 (2002).

60. Cademartiri, L. *et al.* Multigram scale, solventless, and diffusion-controlled route to highly monodisperse PbS nanocrystals. *J. Phys. Chem. B* **110**, 671–673 (2006).

61. Kirkwood, N. *et al.* Finding and Fixing Traps in II-VI and III-V Colloidal Quantum Dots: The Importance of Z-Type Ligand Passivation. *J. Am. Chem. Soc.* **140**, 15712–15723 (2018).

62. Moreels, I. *et al.* Size-tunable, bright, and stable PbS quantum dots: A surface chemistry study. *ACS Nano* **5**, 2004–2012 (2011).

63. Brutchey, R. L. Diorganyl Dichalcogenides as Useful Synthons for Colloidal Semiconductor Nanocrystals. *Acc. Chem. Res.* **48**, 2918–2926 (2015).

64. Ingert, D., Feltin, N., Levy, L., Gouzerh, P. & Pileni, M. P. CdTe quantum dots obtained by using colloidal self-assemblies as templates. *Adv. Mater.* **11**, 220–223 (1999).

65. Rogach, A. L., Eychmüller, A., Hickey, S. G. & Kershaw, S. V. Infrared-emitting colloidal nanocrystals: Synthesis, assembly, spectroscopy, and applications. *Small* **3**, 536–557 (2007).

66. Lin, Z. *et al.* PbTe colloidal nanocrystals: Synthesis, mechanism and infrared optical characteristics. *J. Alloys Compd.* **509**, 5047–5049 (2011).

67. Jung, H. Y. *et al.* Synthesis of quantum-sized cubic ZnS nanorods by the oriented attachment mechanism. *J. Am. Chem. Soc.* **127**, 5662–5670 (2005).

68. Panda, A. B., Acharya, S., Efrima, S. & Golan, Y. Synthesis, assembly, and optical properties of shape- and phase-controlled ZnSe nanostructures. *Langmuir* **23**, 765–770 (2007).

69. Bae, W. K. *et al.* Controlling the influence of Auger recombination on the performance of quantum-dot light-emitting diodes. *Nat. Commun.* **4**, 1–8 (2013).

70. Michalet, X. *et al.* Properties of fluorescent semiconductor nanocrystals and their application to biological labeling. *Single Mol.* **2**, 261–276 (2001).

71. Clarke, M. T. *et al.* Synthesis of super bright indium phosphide colloidal quantum dots through thermal diffusion. *Commun. Chem.* **2**, (2019).